DC-DC converter for high performance hybrid battery applications

Mario Tilocca, Eindhoven University of Technology, Department of Electrical Engineering,
ID 1034263, m.tilocca@student.tue.nl

***Abstract*—In this paper is presented a strategy aimed at the development of a DC-DC converter best suited to operate in an HESS configuration using HP and HE battery types in a Dual-cell architecture for E-scooter application.**
The core feature of the active parallel HESS configuration proposed was represented by the development and testing of a bidirectional DC-DC converter. Which needs to operate either as a boost and either as a buck converter. Through that a 3-phase BLDC was supplied with the energy stored in the UC bank during accelerations of the ES, while it recharged the UC bank during regenerative braking.
It was first simulated the acceleration behavior of an ES. The parameters obtained from that were used for designing the DC-DC converter. According to its requirements a control algorithm was developed in Arduino. Consequently empirical tests were performed to validate the converter and the developed control algorithm.

***Index Terms*—E-Scooter, Hybrid Battery, HESS, Voltage Sensor, Lithium-ion Ultracapacitors, LiFePo4 battery, DC-DC converter, Half Bridge, Buck-Boost, PWM, Control Algorithm.**

I. Introduction

In this paper is discussed about the development of a DC-DC converter which allows to integrate a dual battery architecture in E-scooters (ES) applications. The main contribution is to show an efficient energy management strategy aimed at developing and controlling a DC-DC bidirectional converter. The scope of the converter is to regulate the input and output voltage dynamically. Thus it is possible to ensure a constant output voltage, namely the nominal operating voltage of the BLDC motor used in ES, regardless of the value of the input voltage during ES accelerations. Conversely during regenerative braking the proposed control strategy enables the output voltage to vary according to the state of charge (SoC) of the high power (HP) battery topology. During this process the input voltage supplied is maintained constant throughout the duration in which the employed BLDC motor is operated as a generator. Therefore a research question arises:

What approach should be adopted when developing bidirectional DC-DC allowing to combine a dual battery architecture while ensuring to maintain high performances in ES applications ?

In the following sections of the paper it is discussed about related researches which focused on ES and battery topologies used in light electric vehicles applications. Consequently the methodologies employed and the results obtained during the development and testing of the DC-DC bidirectional converter are examined.

II. Literature research & Background

ES are designed to be a quiet and low vibration vehicle that find their main employment in residential urban areas drastically reducing CO_2 emissions and improving air quality [1] .In recent years with the improvements in the field of a rechargeable batteries it has been possible to sensibly increase the operational range of light E-vehicles where volume constraints play a key role in the design of the E-bikes and ES particularly [2].
Therefore, one of the main challenges is developing a balanced system of different fuel-cell topologies which allows the vehicle to achieve performances and have an autonomy range comparable to scooter mounting an internal combustion engine keeping the total mass of the vehicle approximately the same.
In order to tackle this challenge a possible solution is the development of hybrid energy storage systems (HESSs) [3]. A typical HESS configuration is built using two different topologies of fuel-cells, being able to efficiently combine both High Energy (HE) and High Power (HP) characteristics [4]. In this research paper the goal is being able to develop DC-DC converter suited to operate in a Dual-Cell system which employs Lithium-Ion ultra-capacitors in particular for their HP properties together with Lithium Iron Phosphate (*LiFePo*4) for the HE part.
One of the main focuses is towards the charge/discharge energy efficiency which is one of the main indicators regarding the battery life cycle performance [4]. In order to achieve an higher overall efficiency of the system an important role is played by the handling of the energy during regenerative braking and standstill accelerations where the energy demand is higher compared to cruise speed.
During standstill accelerations the primary source of the energy drawn by the Brush-less DC motor of the vehicle are the lithium-ion ultracapacitors as the overall power demand in order to reach the cruise speed is high. Conversely during the part of the trip at constant speed the LiFePo4 batteries should be the main source of the energy drawn by the BLDC motor as the power demand is low but constant.
During regenerative braking the power flow is reversed, going from the BLDC motor to the fuel-cells. In this scenario the energy should be first directed to the ultracapacitors in order to recharge them [5]. Solely after the ultracapacitors are

fully charged the power should be drawn by the LiFePo4 cathode battery pack as the latter has an higher internal resistance compared to the Lithium-Ion ultracapacitors. Therefore leading to higher losses which can overheat the battery damaging it. Hence in order to minimize the losses a DC-DC converter is placed between the ultracapacitors and the battery pack to allow a bidirectional power flow [6].

III. Methods

A. Acceleration of an E-Scooter

The technology employed in the development of electric scooters have been steadily improving in recent years reaching performances analogous with the ones of internal combustion engine (ICE) scooters.
An important parameter of comparison between the ES and the ICE scooter is represented by the wide open throttle (WOT) behavior of the ES in a standstill acceleration. In order to comprehend this particular behavior a simulation of 500 data points was performed in Matlab. The constant parameters of the ES analyzed are depicted in Table I. Two separate equations were used in order to precisely simulate the behavior of the increase of velocity v_{n+1} of the ES according to: [2]

$$v_{n+1} = v_n + \delta t \cdot (157 - 0.00145 \cdot v_n^2) \tag{1}$$

where v_n is the current velocity, the aforementioned equation can be used to describe the behavior of the ES until it reaches a velocity of 10.8 m/s; afterwards Eq. 2 is used to calculate the next value of the velocity in the simulation [2].

$$v_{n+1} = v_n + \delta t \cdot (7.30 - 0.53 \cdot v_n - 0.00145 \cdot v_n^2) \tag{2}$$

Consequently it is possible to progressively calculate the travelled distance d_{n+1} according to: [2]

$$d_{n+1} = d_n + 0.1 \cdot v_n \tag{3}$$

where, d_n represents the current traveled distance. Since the ES simulation is at WOT it is assumed the acceleration a to be constant as it is depicted in the following equation:

$$a = \frac{2 \cdot d_{tot}}{t^2} \tag{4}$$

where, d_{tot} represents the total distance traveled by the scooter to reach its maximum velocity. Hence, it is possible to determine the behavior of the current drawn from the batteries by the 3-phase BLDC motor, I_{motor} according to Eq. 5. Thus, it is consequently possible to determine the development of traction force of the ES according to Eq. 6 [7].

$$I_{motor} = \frac{a v_n m}{V_{motor}} \tag{5}$$

$$F_{tr} = \frac{V_{motor} I_{motor}}{v_{n+1}} \tag{6}$$

B. Battery Topologies

In the system analyzed HP and HE battery topologies are combined together in an active parallel HESS configuration as it is shown in Fig. 1.

TABLE I
Scooter Simulation constants

Symbol	Variable	Value	Unit
V_m	BLDC motor nominal voltage	48	V
m	total mass of the scooter	180	kg
t	total simulation time	50	s
δt	time sample	0.1	s

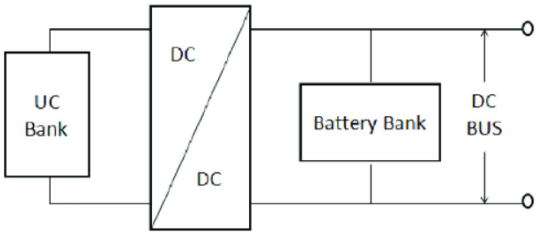

Fig. 1. Active parallel HESS configuration [3]

LiFePo4 cathode battery: Due to its low cost, long durability and more environmental friendly impact compared to cobalt based cathode batteries LiFePo4 have been chosen to be the HE components in the HESS configuration [8]. The specifications of a LiFePo4 fuel-cell are depicted in Table II. In order to meet the DC bus voltage requirements 16 fuel-cells are connected in series thus satisfying the nominal voltage requirement of the BLDC motor of the ES.
Thus the battery bank has a voltage ranging between 58.4 V and 40 V depending on the state of charge SoC of the battery bank.

Lithium-Ion Ultracapacitors: One of the main characteristics of the chosen ultracapacitors is their property to fully discharge in few seconds which makes them best suited to be used as source of power during accelerations of the ES [9]. Their HP characteristics are shown together with the main properties in Table III.
By contrast it is worth to note that the lithium-ion ultracapacitors have a lower energy density compared to the the LiFePo4. In the HESS configuration analyzed 10 Lithium-Ion ultracapacitors fuel-cells were connected in series, with a voltage ranging between 22 V and 38 V depending on the SoC. Which was constantly monitored via a voltage divider connected to the microcontroller.

C. DC-DC Converter

1) Converter Topologies: The main challenge in the development of an HESS configuration is the realization of a bidirectional DC-DC convert. Which allows the power to flow

TABLE II
LiFePo4 characteristics [8]

Name	Value	Unit
Nominal cell voltage	3.2	V
Max charge voltage	3.65	V
Min discharge voltage	2.5	V
Specific Energy	90110	Wh/kg
Energy density	220	Wh/L
Specific Power	200	W/kg
Internal resistance	0.1	Ω

TABLE III
LITHIUM-ION ULTRACAPACITOR SPECIFICATIONS [9]

Name	Value	Unit
Nominal cell voltage	2.2 -3.8	V
Specific Energy	11	Wh/kg
Energy density	19-25	Wh/L
Specific Power	9300	W/kg
Internal resistance	0.13	Ω

TABLE IV
DC-DC CONVERTER CONSTANTS

Symbol	Variable	Value	Unit
V_{DC}	DC bus nominal voltage	48	V
V_c	Ultracapacitors voltage range	22-38	V
f_s	Switching frequency	32000	Hz
I_{DC}	DC bus max current	22.64	A

either from the UC and battery banks to the BLDC motor and either during regenerative braking from the motor to the fuel-cells [10]. Thus creating a power buffer extends the life cycle of either the HP and HE components whilst shrinking the thermal losses.
In this particular case the DC-DC converter must work as a boost converter. Thus regulating the current UC bank voltage to the nominal DC bus voltage, during ES accelerations where the main energy source is provided by the UC bank. Conversely during braking the power recovered should be firstly directed to the UC bank until it is fully charged. Hence during this phase the DC-DC converter has to operate as a buck converter as the DC bus nominal voltage is higher than the maximum UC bank voltage, as it is shown in Table IV.
For the aforementioned reasons the most suitable DC-DC converter for this application is a bidirectional buck-boost half bridge, as shown in Fig. 2.

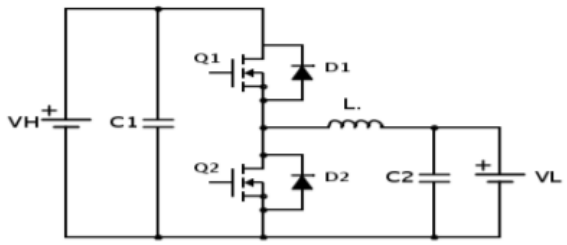

Fig. 2. Bidirectional Buck-Boost Half Bridge [10]

Boost Mode: When working as a boost converter, the power Mosfet Q1 shown in Fig. 2 is switched off for the whole duration of the process, while the power Mosfet Q2 is regulated according to the duty cycle D_{boost} obtained with the following equation:

$$D_{boost} = 1 - \frac{V_c}{V_{DC}} \tag{7}$$

where V_c represents the input voltage, represented by the UC bank voltage and V_{DC} the output voltage represented by the DC bus nominal voltage as it is shown together with the other converter constants in Table IV.

By knowing the duty cycle it is possible to design to determine the required inductance L_1 using the following equation:

$$L_1 = \frac{V_c D_{boost}}{f_s \Delta I_L} \tag{8}$$

where f_s represents the switching frequency and ΔI_L the ripple current which can be obtained according to Eq. 9:

$$\Delta I_L = \frac{0.35 \cdot V_{DC} \cdot I_{DC}}{V_c} \tag{9}$$

where it is assumed that the ripple current is equal to 35% of the maximum output current I_{DC} drawn by the BLDC motor. Moreover it is possible to calculate the required output capacitance C_1 as shown in Eq. 10 where ΔV_{rip} represents the voltage ripple which is assumed to be maximum 1% of the total output voltage and it is calculated according to Eq. 11.

$$C_1 = \frac{I_{DC} D_{boost}}{f_s \Delta V_{rip_B}} \tag{10}$$

$$\Delta V_{rip_B} = 0.01 \cdot V_{DC} \tag{11}$$

Buck Mode: During regenerative braking it is assumed that the UC bank is empty as the energy in it should have been used previously during the acceleration phase.
Therefore the DC-DC converter works in buck mode in order to recharge the UC bank. Assuming a 100% efficiency it can be assumed that the power in input P_{in} is equal to the power in output P_{out} as shown in the following equations:

$$P_{in} = V_{DC} I_{DC} \tag{12}$$

$$P_{in} = P_{out} \tag{13}$$

by knowing the power in output it is possible to calculate the current which is drawn by the UC bank I_c during regenerative braking as shown in the following equation:

$$I_c = \frac{P_{out}}{V_c} \tag{14}$$

During this phase the power Mosfet Q2 is switched off, while by knowing the duty cycle D_{buck} as it is shown in Eq.15 of the power Mosfet Q1 showed in Fig. 2, it is possible to calculate the required inductance L_2 through Eq. 16.

$$D_{buck} = \frac{V_c}{V_{DC}} \tag{15}$$

$$L_2 = \frac{V_c \cdot (1 - D_{buck})}{2 \cdot f_s I_c} \tag{16}$$

Moreover the required output capacitance C_2 can be calculated according to the following equation:

$$C_2 = \frac{D_{buck} I_c}{f_s \Delta V_{rip_b}} \tag{17}$$

where ΔV_{rip_b} represents the voltage ripple which is estimated to account for 1% of the UC bank voltage as shown in the equation below.

$$\Delta V_{rip_b} = 0.01 \cdot V_c \tag{18}$$

D. Microcontroller Implementation & PWM Algorithm

In order to monitor the SoC of the UC bank and the voltage being supplied to or drawn by the DC bus two voltage sensors were be used. Hence two voltage dividers were directly implemented on the PCB which was connected with the employed Arduino Mega 2560. The chosen microcontroller can sense a maximum voltage of 5 V, any value above might cause irreparable damage. Therefore the resistors employed had a value of 1 kΩ and 12 kΩ respectively. Thus the microcontroller could safely sense voltages up to 65 V while maintaining an optimal current of 3.8 mA. By constantly being updated regarding the voltage of the UC bank and DC bus it was possible to estimate the SoC. Based on current SoC of the UC and DC bus the duty cycle D_{boost} of the power Mosfet Q2 was constantly adapted by sending a new pulse width modulation (PWM). As more power during accelerations is being drawn by the BLDC motor the voltage V_c of the UC bank is reduced and therefore the duty cycle D_{boost} increased.
Conversely during regenerative braking the duty cyle D_{buck} was updated according to voltage of the UC bank V_c representing its SoC. Which gradually increased as the supercapacitors were being recharged.

IV. Results & Discussion

A. Acceleration of an E-scooter

By applying Eq.1 and Eq.2 into the Matlab tool the behavior of the velocity of the ES at WOT can be obtained as it is shown in Fig.3. In this figure it is shown how the maximum velocity obtained is around 48 km/h, which accurately represents the empirical behavior of scooters. Consequently, by applying Eq.3 and Eq.4 it was found that the acceleration a of the ES at WOT is equal to 0.483 m/s^2. In Fig.4 it is shown the

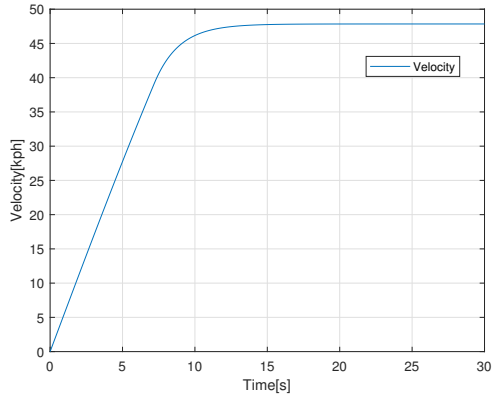

Fig. 3. Full power acceleration of ES

behavior of the current drawn by the BLDC motor of the ES which was obtained by applying Eq.5. It is worth mentioning that the behavior of velocity, shown in Fig.3, and the behavior of the motor current, shown in Fig. 4, are similar as they are both influenced by the acceleration a.

By comparing the velocity of the scooter and the current

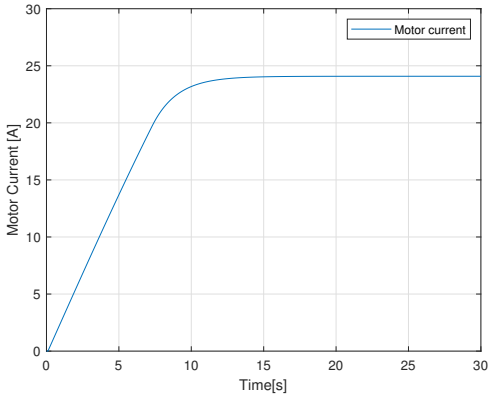

Fig. 4. Current drawn by the scooter motor during acceleration time

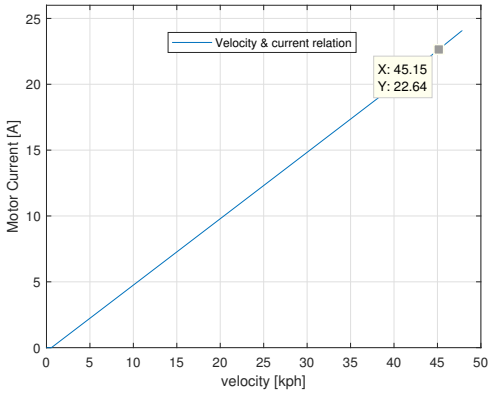

Fig. 5. Current drawn by the scooter motor with respect to velocity

drawn by its motor as it is shown in Fig.5 it is worth noting that they have a linear relation; furthermore from the aforementioned graph it was possible to determine the current drawn by the motor at 45 km/h which is the speed limit at which the scooters are allowed to drive in most EU countries. The value obtained from this graph was used as maximum motor current I_{DC} in the DC-DC converter parameters calculations. Moreover by applying Eq.6 it was possible to simulate the

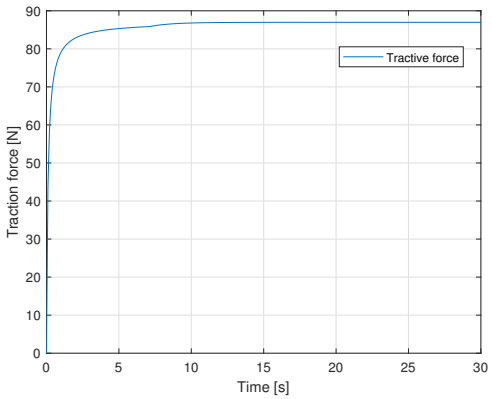

Fig. 6. Traction force behavior of ES at full power acceleration

TABLE V
DC-DC CONVERTER PARAMETERS

Symbol	Variable	Value	Unit
C_1	Boost output capacitance	798	μF
C_2	Buck output capacitance	5600	μF
L_1	Inductance boost	21.5400	μH
L_2	Inductance buck	1.4498	μH

behavior of the traction force F_{tr} of the ES as shown in Fig.6, it is worth noting that the force reaches in 10 seconds its peak value which is 87 N and it behaves steadily afterwards. The rapid growth above 80 N in less than 2 seconds has to be addressed to the constant acceleration at which the scooter is traveling. Consequently as the velocity of the scooter is higher than 10.8 m/s it slows its growth until it steadily increase to reach 87 N. Furthermore it is important to mention that the values of the traction force obtained in the simulation are similar with discrepancy of 0.34% to the gathered empirical data of a similar ES which reaches a speed of 35 km/h with a traction force of 86.7 N [7].

B. DC-DC Converter

In order to realize the DC-DC converter PCB using the software Eagle it was first needed to calculate the boost capacitance C_1 and the buck capacitance C_2 following Eq.10 and Eq.17 respectively as it is shown in TableV.
Furthermore the respective inductors L_1 for the boost mode and L_2 for the buck mode were calculated according to Eq.8 and Eq.16. However since it is possible to mount only one inductor in the chosen design it was decided to build the inductor designed for the boost mode as it is larger than the minimal one needed for the buck mode as it is shown in Table V. In Fig.7 it is shown the circuitry schematics developed through the software Eagle, it was decided to use to satisfy the buck capacitance C_2, 3 parallel connected ECA1JHG222 electrolytic capacitors with 2200 μF capacitance each. Whilst 2 parallel connected MCKSK100M471J32S electrolytic capacitors with 270 μF capacitance each for the boost capacitance C_1.
The power Mosfet employed was the FQP85N06due to its high switching properties and its reliability at high voltages and currents. Moreover the FQP85N06 power Mosfets will receive the boosted PWM signal from the IR2110 gate driver which was connected directly to the Arduino Mega 2560. The final layout of the 2 layer PCB board designed is presented in Fig.8. The board high power traces were designed to be 0.018 mm thick and 7.62 mm wide in order to resist to a current up to 18 A. Whilst the traces concerning the gate driver and voltage dividers were designed to be 0.635 mm wide being resistant to a current up to 2.7 A. Furthermore two ground planes were designed having an minimal isolation of 1.27 mm from each trace.

V. TESTING

The proposed DC-DC converter design and control algorithm were empirically tested. In the experimental setup in addition to the Arduino Mega 2560 and the assembled PCB a 94 Ω resistor was employed as load to dissipate the

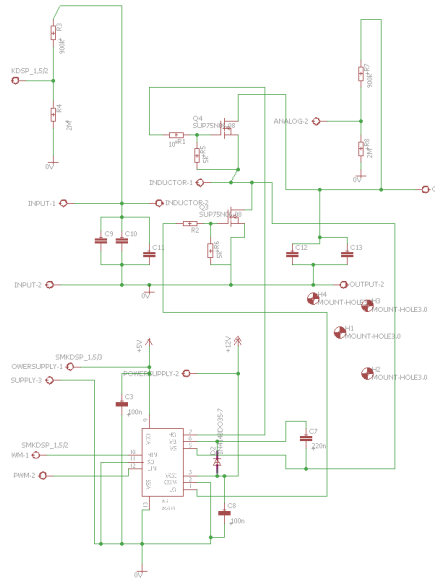

Fig. 7. Bidirectional buck-boost half bridge Eagle schematic

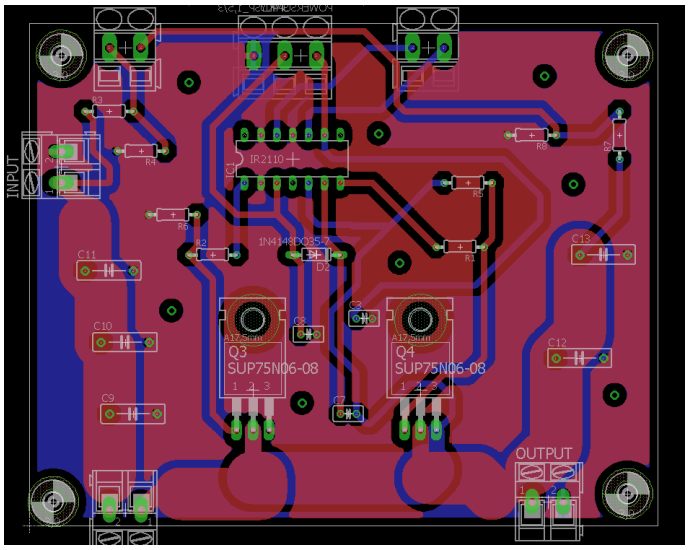

Fig. 8. Bidirectional buck-boost half bridge Eagle designed PCB

power while a DC voltage source was used to supply power to the circuit. Two external auxiliary DC voltage sources were employed in order to power the IR2110 gate driver. Furthermore the switching frequency was increased from 32 kHz to 62.5 kHz in order to enable higher reliability and lower losses.
Before tests involving the lithium-ion ultracapacitors could be conducted it was first tested that the converter worked in boost and buck mode with fixed duty cycles D_{boost} and D_{buck}. In order to achieve the correct values the function which calculated the duty cycle in Arduino had to be adjusted and tuned. As these experiments were successful the control algorithm aimed at dynamically update the duty cycle could be tested. During Boost operation the DC-DC converter input voltage was gradually manually decreased ranging from 38 V to 22 V as it is shown in Fig.9.

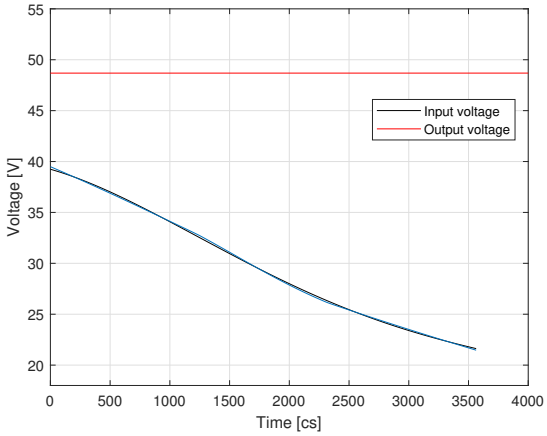

Fig. 9. DC-DC converter input and output voltage fitted curves behavior during Boost operation

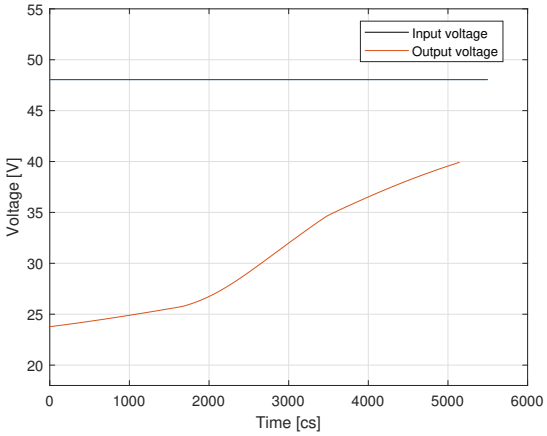

Fig. 10. DC-DC converter input and output voltage fitted curves behavior during Buck operation

This was aimed at simulate the behavior of the ultracapacitors bank whose voltage is dropped as its SoC shrinks.
The output voltage behavior remained steady throughout the entire experiment as it is shown in Fig.9.
In this figure the behavior of the data recorded through the microcontroller has been processed in Matlab to obtain the fitted curves of the behavior of the input and output voltage.
Conversely during buck operation as the power flow is reversed the input voltage is maintained steady at 48 V while the supercapacitors were being recharged. An offset 12.727% higher with respect to the initial voltage during buck operation (22 V) in the Arduino resolution was recorded as it is presented in Fig.10.
Thus during buck operation the UC bank was overcharged despite an input current of 0.82 A. Consequently this led to damaging the UC bank. However the behavior of the output voltage during buck operation shown in Fig. 10 followed the theoretical expectations as it gradually increased as the SoC of the UC bank incremented.
Hence, despite the boost operation of the converter could not be tested with the UC bank its control strategy has been successful as the behavior of the input voltage is shown in Fig.9.
As in order to obtain a steady output voltage behavior the duty cycle D_{boost} was successfully dynamically adjusted.

VI. Conclusion & Reflection

In this paper the behavior of an ES during full power acceleration, an HESS configuration employing a Dual-Cell fuel battery type together with a bidirectional DC-DC converter and its control and modulation strategy were presented. It has been shown that a correct implementation of the ES model has a crucial impact when determining the core parameters of the DC-DC converter. Furthermore it has been demonstrated that the proposed converter circuitry satisfied the theoretical assumptions when empirically tested. Moreover, despite the PWM control algorithm had to be adjusted and adequately tuned during the execution of the testing phase it can be said to be effective. Although the recorded data presented discrepancies with the expected values the executed tests were successful. Thus, it can be said that the initial research question is answered. However several improvements could be still achieved. Namely due to the inaccuracies regarding the SoC of the UC bank an improved control strategy could be formulated. The main focus should be on developing and successfully implementing an algorithm where the SoC of the UC bank is accurately monitored. Furthermore it should be able to safely interrupt the power flow towards the UC bank in buck operation in case it is satisfactorily recharged.

References

[1] T. Kim, O. Vodyakho, & J. Yang, *Fuel cell hybrid electric scooter*, IEEE Industry applications magazine, mar — apr 2011.
[2] James Larminie, John Lowry *Electric Vehicle Technology Explained*, John Wiley & Sons Ltd, The Atrium, Southern Gate, Chichester, West Sussex PO19 8SQ, England, 2003.
[3] Wang, Yanzi and Wang, Weida and Zhao, Yulong and Yang, Lei and Chen, Wenjun,*A Fuzzy-Logic Power Management Strategy Based on Markov Random Prediction for Hybrid Energy Storage Systems*, Energies, 01-2016, 10.3390/en9010025.
[4] Omar, Noshin & Kurtulus, Can & Krabb, Peter & Hennige, Volker & Rsnen, Mika & Salminen, Justin & Nuutinen, Matti & Grosch, Joschua & Jank, Michael & Teuber, Erik & Lorentz, Vincent & Petit, Martin & Martin, Joseph & Silvi, Jean-Louis & Widanage, Dhammika. *SuperLIB : Smart Battery Management of a Dual Cell Architecture for Electric Vehicles*, 2014.
[5] Noshirwan K. Medora & Alexander Kusko. *Battery Management for Hybrid Electric Vehicles using Supercapacitors as a Supplementary Energy Storage System*. IEEE 2012.
[6] Yuhimenko, Vladimir & Lerman, Chaim Kuperman, Alon. *DC Active Power Filter based Hybrid Energy Source for Pulsed Power Loads*. IEEE Journal of Emerging and Selected Topics in Power Electronics. 2015.
[7] Robin Weijers, Bob Molenaar, Steven Wilkins, Frans van de Weijdeven, *ACE internship: SmartBike2*, TNO, ACE, 1-03-2019.
[8] Nomo Co Group Limited, *http://www.smart-solar-lights.com/info/specification-of-the-lithium-iron-phosphate-l-20037899.html*, 20-04-2019.
[9] Fleurbaey, Karel & Ronsmans, Jan & de Hoog, Joris & Nikolian, Alexandros & Timmermans, Jean-Marc & Omar, Noshin & Van den Bossche, Peter & Van Mierlo, Joeri, *Lithium-ion Capacitor - Electrical and thermal characterization of Advanced Rechargeable Energy Storage Component*, 2014.
[10] Sureshkumar B. Tank, Kelvin Manavar, Nitin Adroja, Electrical Engineering Department, Atmiya Institute of Technology & Science, Rajkot *Non-Isolated Bi-directional DC-DC Converters for Plug-In Hybrid Electric Vehicle Charge Station Application*, National Conference on Emerging Trends in Computer, Electrical & Electronics (ETCEE-2015).